Reproduction Quality Notice

This document is part of the Air Technical Index [ATI] collection. The ATI collection is over 50 years old and was imaged from roll film. The collection has deteriorated over time and is in poor condition. DTIC has reproduced the best available copy utilizing the most current imaging technology. ATI documents that are partially legible have been included in the DTIC collection due to their historical value.

If you are dissatisfied with this document, please feel free to contact our Directorate of User Services at [703] 767-9066/9068 or DSN 427-9066/9068.

Do Not Return This Document To DTIC

Disreg Ard Reel C-53
with ATI No 6409.
6409 is OKay

REEL - C

168

A.T.I.

6409

ARR No. LAK22b

NATIONAL ADVISORY COMMITTEE FOR AERONAUTICS

WARTIME REPORT

ORIGINALLY ISSUED
December 1944 as
Advance Restricted Report LAK22b

A SOLUTION OF THE DIRECT AND INVERSE POTENTIAL PROBLEMS FOR ARBITRARY CASCADES OF AIRFOILS

By William Mutterperl

Langley Memorial Aeronautical Laboratory
Langley Field, Va.

NACA

WASHINGTON

NACA ARR No. I4K22b

NATIONAL ADVISORY COMMITTEE FOR AERONAUTICS

ADVANCE RESTRICTED REPORT

A SOLUTION OF THE DIRECT AND INVERSE POTENTIAL PROBLEMS FOR ARBITRARY CASCADES OF AIRFOILS

By William Mutterperl

SUMMARY

Solutions of the direct potential problem for a cascade - namely, to find the potential flow past an arbitrary cascade of airfoils - and of the inverse problem - namely, to find an airfoil having a prescribed velocity distribution in cascade - are presented. The methods used represent the extension to cascades of the Cartesian mapping function method of conformal transformation. Numerical examples of the direct and inverse methods are given. The numerical labor required is conservatively estimated as double that involved for isolated airfoils by the corresponding methods.

INTRODUCTION

The potential flow through a cascade of airfoils bears approximately the same relation to the real flow through axial and through some types of centrifugal turbines and compressors that the potential flow about isolated airfoil sections bears to the real flow about airplane wings. A knowledge of the potential flow through a cascade is therefore recognized as basically important for the aerodynamic study and design of such machines. The relative difficulty of making measurements on airfoils in cascade further accentuates the necessity of a potential-flow solution.

As was the case for isolated airfoils, there are two potential problems for the cascade that are of primary practical importance. The first, or direct problem, is that of determining the potential flow past a given arbitrary cascade of airfoils. The second, or inverse problem, is that of deriving an airfoil section to have a prescribed surface pressure distribution in cascade.

The theoretical methods available for the solution of these problems are, roughly speaking, of three kinds, namely:

(1) Methods that regard a blade of the cascade as an isolated airfoil operating in a flow composed of a free-stream velocity and a disturbance velocity due to all the other blades of the cascade. The method applies best to cascades of thin airfoils with small solidity. (See reference 1, p. 70, and bibliography contained therein.)

(2) Stream-filament methods, which regard the space between the blades of the cascade as channels of varying area but in which the streamlines are uniform or of simple curvature. These methods apply best to cascades of high solidity in which, moreover, the flow is smooth (shock free) at entrance.

(3) Methods based on conformal transformation of the cascade. These methods may be subdivided as follows:

(a) Methods based on the concept of the equivalent cascade of flat plates; that is, the cascade of flat plates with spacing equal to that of the given cascade, with blade angle equal to the zero-lift angle of the given cascade, and into which the given cascade can be transformed conformally. Extensive use of this concept is made in reference 1, on the basis of which are given approximate solutions of the direct and inverse problems for cascades of various types of shape and for various ranges of solidity. The solutions are approximate mainly because of the methods given for the determination of the equivalent cascade from the given cascade or vice versa.

(b) Particular conformal transformations that yield special classes of shape for which the flow can be calculated exactly (such as those of reference 1, p. 55, and reference 2).

(c) Exact methods for arbitrary airfoils or pressure distributions in cascade, such as those that exist for isolated airfoils. For this purpose, Wsinig (reference 1, p. 90) utilizes the basic known transformation from a cascade of flat plates to a single circle. By this transformation, the given cascade transforms to a near circle. The near circle, p'-plane, is then

transformed to a circle, p-plane, by a modification of the Theodorsen-Garrick procedure (reference 3) consisting in the use of log dp'/dp instead of log p'/p as the mapping function. The transformation of the given cascade to the near circle appears to be much more laborious and the near circle much more different from a circle than is the case for the transformation of isolated airfoils. This general procedure has recently been treated in reference 4. A similar method has also been used in a British paper by A. R. Howell. The basic transformation that reduces the given cascade to a single shape is taken as $\zeta = \tanh z$, where z is the physical plane. Inasmuch as the resulting ζ-plane shape is not of near-circle type, several Joukowski transformations are applied to produce a near circle. The transformation from near circle to circle is then accomplished by the Theodorsen-Garrick method. This method, too, involves an excessive amount of numerical labor.

In the present paper, the Cartesian mapping function method of reference 5 is extended to the solution of the direct and inverse potential problems for arbitrary cascades of airfoils. After an exposition of some basic properties of the Cartesian mapping function for cascades, procedures are given for the solution of the direct and inverse problems. The procedures are then illustrated by numerical examples.

Acknowledgment is made to Mrs. Lois Evans Doran of the computing staff of the Langley full-scale tunnel for her assistance in making the calculations.

SYMBOLS

$z = x + iy$	plane of cascade of airfoils
$\zeta = \xi + i\eta$	plane of cascade of straight lines
p	plane of unit circle
φ	central angle of circle
Δx	component of Cartesian mapping function (CMF) parallel to chord
Δy	component of Cartesian mapping function perpendicular to chord
τ	displacement constant for locating airfoil

β blade angle of cascade, measured between chord line and normal to cascade direction

K parameter of transformation from cascade of straight lines to unit circle

β_K central angle of unit circle that corresponds to extremity of flat plate in cascade (equation (7))

c chord

σ solidity $\left(\frac{\text{chord}}{\text{spacing}}\right)$

σ_l solidity of cascade of straight lines

$C = 2\sqrt{\cos^2\beta + \sinh^2 K}$ (equation (12))

S adjustment constant (equations (13) to (15))

v_z velocity at airfoil surface

v_p velocity at surface of unit circle

V relative mean velocity in physical plane

W complex potential in circle p-plane

Γ circulation

λ relative stream angle (See fig. 5.)

λ_K $\tan \lambda_K = \tan \lambda \tanh K$ (equation (27))

λ_{K_1} corresponds to ideal stream angle (equation (32))

φ_{TK} $\tan \varphi_{TK} = \dfrac{\tan \varphi_T}{\tanh K}$ (See equation (21))

l lift force per unit length on airfoil in cascade, perpendicular to relative mean velocity

ρ density

c_l lift coefficient $\left(\frac{l}{\frac{1}{2}\rho V^2 c}\right)$

α angle of attack, measured between mean relative stream direction and chord line

β_0 zero lift angle, angle of attack for zero lift

δ angle of deviation of relative flow from leading- or trailing-edge direction of airfoil (See fig. 5.)

k denominator of equation (30)

$$\left[(\sin^2\varphi + \sinh^2\chi)\sqrt{\left(\frac{d\xi}{d\rho} - \frac{d\Delta x}{d\varphi}\right)^2 + \left(\frac{d\Delta y}{d\varphi}\right)^2}\right]$$

P pressure coefficient $\left[1 - \left(\frac{v_z}{V}\right)^2\right]$

Subscripts:

N leading edge (nose)

T trailing edge

u upstream

d downstream

APPLICATION OF CARTESIAN MAPPING FUNCTION TO CASCADES

The general scheme of application of the CMF to cascades of airfoils was indicated in reference 5. Basically, the method consists in relating conformally the points of an airfoil in cascade to the points of its extended chord line by means of the vector difference between pairs of corresponding points. This vector difference, called the Cartesian mapping function (CMF), is a function of position in any of the mapping planes used. It is regular and periodic in the entire region outside the airfoil boundaries, in the corresponding region outside the straight lines, and is regular in the entire region outside the single unit circle into which the preceding regions can be conformally transformed. Instead of the simple Joukowski transformation from the isolated straight line to the circle, however, as was used for the isolated airfoil, the more complicated but well-known transformation from

a cascade of straight lines to a circle is now necessary to express the CMF as a regular function outside the circle. Various preparatory details of these transformations are next set down, prior to a discussion of the general direct and inverse problems for cascades.

CMF for cascades.- The CMF from the cascade of airfoils to the cascade of flat plates is taken as $z - \zeta$. (See fig. 1.) Because $z - \zeta$ is regular everywhere outside the cascade of flat plates - in particular, in the infinite strip outside one plate that maps into the entire region outside the unit circle - it is regular everywhere outside the circle and is therefore expressible by the inverse power series[1]

$$z - \zeta = \sum_{0}^{\infty} \frac{c_n}{p^n} \tag{1}$$

On the corresponding boundaries of airfoil, flat plate, and circle

$$z - \zeta = (x - \xi) + iy$$

$$\equiv \Delta x + i\Delta y \tag{2a}$$

and

$$p = e^{i\Phi} \tag{2b}$$

Substitution of equations (2a) and (2b) in equation (1), with $c_n = a_n + ib_n$, gives for Δx and Δy the conjugate Fourier series

$$\Delta x(\Phi) = a_o + \sum_{1}^{\infty} a_n \cos n\Phi + \sum_{1}^{\infty} b_n \sin n\Phi \tag{3}$$

[1]The mapping function chosen is periodic with respect to the same strip in the ζ-plane that maps into the entire p-plane region outside the unit circle. The necessity of introducing a cut in the infinitely many-sheeted p-plane is thereby eliminated.

$$\Delta y(\varphi) = b_o + \sum_{1}^{\infty} b_n \cos n\varphi - \sum_{1}^{\infty} a_n \sin n\varphi \qquad (4)$$

The corresponding integral relations between Δx and Δy are the same as in reference 5.

Flat-plate transformation.- The transformation from the cascade of flat plates, ζ-plane, to a single unit circle, p-plane, which makes the CMF a function of the central angle φ of the circle, is (fig. 2 and references 1 and 6)

$$\zeta - \tau = e^{-i\beta} \log_e \frac{e^K + p}{e^K - p} + e^{i\beta} \log_e \frac{p + e^{-K}}{p - e^{-K}} \qquad (5)$$

This transformation is periodic in ζ with a cascade spacing (period) of 2π. The points $\zeta = \pm\infty$ correspond to $p = \pm e^K$. The constant displacement τ is inserted for future convenience in locating the cascade of airfoils. The correspondence between points on the flat plate and points on the circle is obtained by substituting $\zeta = \xi + i\eta$ and $p = e^{i\varphi}$ in equation (5). The result is

$$\left.\begin{aligned} \xi &= \tau + \cos\beta \log_e \frac{\cosh K + \cos\varphi}{\cosh K - \cos\varphi} + 2 \sin\beta \tan^{-1} \frac{\sin\varphi}{\sinh K} \\ \eta &= 0 \end{aligned}\right\} \qquad (6)$$

The angles β_K, $\beta_K + \pi$ that correspond to the extremities of the flat plate are obtained by maximizing ξ in equation (6) with respect to φ. The resulting condition is

$$\tan\beta_K = \tan\beta \tanh K \qquad (7)$$

Substitution of equation (7) in equation (6) gives the solidity $\sigma_\zeta = \dfrac{\xi_{max} - \xi_{min}}{2\pi}$ of a cascade of straight

lines in terms of the blade angle β and parameter K as

$$\sigma_l = \frac{2}{\pi}\left(\cos\beta \log_e \frac{\sqrt{\sinh^2 K + \cos^2\beta} + \cos\beta}{\sinh K} + \sin\beta \tan^{-1}\frac{\sin\beta}{\sqrt{\sinh^2 K + \cos^2\beta}}\right) \tag{8}$$

It is remarked that, in the applications which are to be given, values of ζ corresponding to selected Φ-values will be determined from equation (6). The relatively more difficult inverse calculations of Φ for a given ζ, or the still more difficult calculation of p for a given ζ by equation (5), will not be necessary. Therein lies the essential numerical simplicity of the CMF method for cascades.

Airfoil position and adjustments in terms of CMF.- The coordinates x, y of the airfoil corresponding to the points at the angular positions Φ on the unit circle are obtained from equations (2a) and (6), as

$$x = \tau + \cos\beta \log_e \frac{\cosh K + \cos\Phi}{\cosh K - \cos\Phi} + 2\sin\beta \tan^{-1}\frac{\sin\Phi}{\sinh K} + \Delta x(\Phi) \tag{9}$$

$$y = \Delta y(\Phi) \tag{10}$$

As was the case for isolated airfoils, it will be necessary to find for cascades the points on the circle corresponding to the chordwise extremities of the airfoil. The abscissa x in equation (9) is therefore maximized with respect to Φ. The resulting condition is

$$\frac{d\Delta x}{d\Phi} = \frac{C \sin (\Phi - \beta_K)}{\sinh^2 K + \sin^2 \Phi} \tag{11}$$

where

$$C = 2\sqrt{\cos^2 \beta + \sinh^2 K} \tag{12}$$

and β_K is defined by equation (7). Equation (11) is solved (graphically) for the angles Φ_N and Φ_T corresponding to the leading and trailing edges of the airfoil (defined as the extremities of the airfoil abscissas).

The solution of equation (11) will usually be carried out in connection with such an adjustment of the airfoil that the extremities are symmetrically located and add up to a desired chord (solidity). The adjustments are similar to the horizontal and vertical stretchings for the isolated airfoil. The horizontal stretching adjustment consists in finding the length of straight line, that is, K, by equation (8) since β is the known angle of the airfoil chord line, which with a given $\Delta x(\Phi)$ will place the airfoil extremities at $\pm\frac{c}{2} = \pm\pi\sigma$, where σ is the given solidity and c is the airfoil chord. The vertical stretching adjustment consists in finding, for a given length and angle of straight line, the factor S by which to multiply a known $\Delta x(\Phi)$ in order that the resulting airfoil will have its extremities at $\pm\frac{c}{2} = \pm\pi\sigma$, where again σ is the desired solidity. The equations for these adjustments are obtained by equating the abscissas of the airfoil extremities to their desired values; that is,

$$x_N = \frac{c}{2} = \pi\sigma$$

$$= \tau + \cos\beta \log_e \frac{\cosh K + \cos \Phi_N}{\cosh K - \cos \Phi_N}$$

$$+2 \sin\beta \tan^{-1} \frac{\sin \Phi_N}{\sinh K} + S\Delta x_N \tag{13}$$

$$x_T = -\frac{c}{2} = -\pi\sigma$$

$$= \tau + \cos\beta \log_e \frac{\cosh K + \cos \Phi_T}{\cosh K - \cos \Phi_T}$$

$$+ 2 \sin\beta \tan^{-1} \frac{\sin \Phi_T}{\sinh K} + S\Delta x_T \qquad (14)$$

In addition, equation (11) for the airfoil extremities is rewritten as

$$S\frac{d\Delta x}{d\Phi} = \frac{C \sin(\Phi - \beta_K)}{\sinh^2 K + \sin^2 \Phi} \qquad (15)$$

Subtraction of equation (14) from equation (13) yields

$$2\pi\sigma = \cos\beta \log_e\left(\frac{\cosh K + \cos \Phi_N}{\cosh K - \cos \Phi_N}\right)\left(\frac{\cosh K - \cos \Phi_T}{\cosh K + \cos \Phi_T}\right)$$

$$+ 2 \sin\beta\left[\tan^{-1}\left(\frac{\sin \Phi_N}{\sinh K}\right) - \tan^{-1}\left(\frac{\sin \Phi_T}{\sinh K}\right)\right] \qquad (16)$$

$$+ S(\Delta x_N - \Delta x_T)$$

Addition of equations (13) and (14) yields

$$-2\tau = \cos\beta \log_e\left(\frac{\cosh K + \cos \Phi_N}{\cosh K - \cos \Phi_N}\right)\left(\frac{\cosh K + \cos \Phi_T}{\cosh K - \cos \Phi_T}\right)$$

$$+ 2 \sin\beta\left[\tan^{-1}\left(\frac{\sin \Phi_N}{\sinh K}\right) + \tan^{-1}\left(\frac{\sin \Phi_T}{\sinh K}\right)\right] \qquad (17)$$

$$+ S(\Delta x_N + \Delta x_T)$$

In the horizontal stretching adjustment, equations (15) and (16) with $S = 1$ are solved simultaneously for K, Φ_N, and Φ_T, with β and σ given. In the vertical stretching adjustment, equations (15) and (16) are solved simultaneously for S, Φ_N, and Φ_T, with K, β, and σ given. Finally, equation (17) is solved for τ.

Velocity and pressure distributions.- Once the conformal correspondence between a cascade of airfoils and the unit circle has been obtained - that is $\Delta x(\Phi)$, $\Delta y(\Phi)$, K, Φ_N, and Φ_T - the velocity at the airfoil surface is given as usual by the product of the velocity at the corresponding point of the circle and the stretching factor from the circle to the airfoil, as

$$v_s(x,y) = \frac{v_p(\Phi)}{\left|\frac{dz}{dp}\right|} \tag{18}$$

The velocity in the circle plane is that due to a superposition of sources and vortices at the points $p = \pm e^{\pm K}$ (fig. 3), which reproduce the desired flow conditions at $\pm\infty$ in the physical plane and which maintain the unit circle, and hence the cascade of airfoils, as streamlines (reference 6). The effect of a source at $p = e^{K}$ is to produce a velocity at $z = \infty$ from right to left of magnitude $\frac{m}{2\pi}$; that is, the complex velocity is $-\frac{m}{2\pi}e^{i\beta}$, where m is the total flux of the source. This fact is evident from the complex potential for a source and the transformation (equation (5)) between p-plane and ζ-plane. The additional effect of an equal source at the image point $p = e^{-K}$, together with an equal sink at the origin, is to make the circle (hence the cascade of flat plates and airfoils) a streamline while maintaining the same flow condition at infinity. Similarly, the effect of a counterclockwise vortex at $p = e^{\Delta}$ is to produce a downward velocity at $z = \infty$ of magnitude $\frac{k}{2\pi}$; that is, the complex velocity is $\frac{ik}{2\pi}e^{i\beta}$, where k is the vortex circulation. The additional effect of an equal and opposite vortex at $p = e^{-K}$ is to make the circle a streamline.

If the flow conditions at infinity in the physical plane are taken as consisting of a mean velocity V at

angle λ (fig. 1), on which is superimposed the tangential velocity $\pm\frac{\Gamma}{4\pi}$ at $z = \mp\infty$ to correspond to the circulation about the airfoil Γ (positive clockwise), the complex potential in the circle plane is that due to the system of sources, sinks, and vortices indicated in figure 3; namely,

$$W = -V \cos\lambda \log\left(\frac{p + e^{K}}{p - e^{K}}\right)\left(\frac{p + e^{-K}}{p - e^{-K}}\right)$$

$$-iV \sin\lambda \log\left(\frac{p - e^{K}}{p + e^{K}}\right)\left(\frac{p + e^{-K}}{p - e^{-K}}\right)$$

$$+i\frac{\Gamma}{4\pi} \log\left(\frac{p + e^{-K}}{p + e^{K}}\right)\left(\frac{p - e^{-K}}{p - e^{K}}\right) \qquad (19)$$

The circulation Γ is fixed by the Kutta condition of smooth flow at the trailing edge in the physical plane or $dW/dp = 0$ at $p = e^{i\Phi_T}$ in equation (19). The resulting circulation is

$$\Gamma = 4\pi V \frac{\sqrt{\sin^2\Phi_T + \sinh^2 K}}{\sinh K \cosh K} \sin\left(\Phi_{TK} - \lambda\right) \qquad (20)$$

where

$$\tan\Phi_{TK} \equiv \frac{\tan\Phi_T}{\tanh K} \qquad (21)$$

It is noted here that the resultant force on an airfoil of the cascade is, by elementary cascade theory,

$$l = \rho V \Gamma \qquad (22)$$

where l acts perpendicular to the relative mean velocity V. The lift coefficient of the section based on the relative mean velocity V is therefore, with $c = 2\pi\sigma$,

$$c_l \equiv \frac{l}{\frac{1}{2}\rho V^2 c} = \frac{\Gamma}{\pi V c} \tag{23}$$

Setting

$$\lambda \equiv \alpha + \beta \tag{24a}$$

and

$$\varphi_{TK} \equiv \pi - \beta_T + \beta \tag{24b}$$

and from equations (20) and (23), the lift coefficient of an arbitrary airfoil in cascade is

$$c_l = \frac{4}{\sigma} \frac{\sqrt{\sin^2\varphi_T + \sinh^2 K}}{\sinh K \cosh K} \sin(\alpha + \beta_T) \tag{25}$$

The angles α and β_T are, respectively, the mean relative stream angle of attack and the zero-lift angle measured from the airfoil chord line. Equation (25) is seen to be similar in form to the corresponding equation for isolated airfoils, to which it reduces in the limit of zero solidity.

With the circulation of equation (20), the velocity distribution on the unit circle is obtained by differentiation of equation (19) and substitution of $p = e^{i\varphi}$. The result is

$$\frac{v_n(\varphi)}{V} = 2 \frac{\sqrt{\cos^2\lambda + \sinh^2 K}}{\sin^2\varphi + \sinh^2 K} \left[\sin(\varphi - \lambda_K) - \sin(\varphi_T - \lambda_K)\right] \tag{26}$$

where

$$\tan \lambda_K \equiv \tan \lambda \tanh K \tag{27}$$

The stretching factor $\left|\frac{d\zeta}{dp}\right|$ from the circle plane to the flat-plate cascade plane is obtained by differentiation of equation (5). The result is equal to $v_p(\varphi)$ (equation (26)) with the circulation term omitted and $\lambda = \beta$. (The transformation (5) can, in fact, be derived (reference 6) by a hydrodynamical argument similar to that leading to equation (19).) Thus,

$$\left[\frac{d\zeta}{dp}\right] = 2\sqrt{\cos^2\beta + \sinh^2 K}\,\frac{\sin(\varphi - \beta_K)}{\sin^2\varphi + \sinh^2 K} \tag{28}$$

where β_K has been defined by equation (7), and $\left[\frac{d\zeta}{dp}\right] = \pm\left|\frac{d\zeta}{dp}\right|$ depending on the sign of $\varphi - \beta_K$.

The over-all stretching factor $\left|\frac{dz}{dp}\right|$ from the circle plane to the physical plane is obtained by differentiation of equation (2a),

$$z - \zeta = \Delta x + i\Delta y$$

$$\frac{dz}{dp} = \frac{d\zeta}{dp} + \frac{d\Delta x}{dp} + i\frac{d\Delta y}{dp}$$

$$= \left[\frac{d\zeta}{dp}\right] ie^{-i\varphi} + \frac{d\Delta x}{ie^{i\varphi}d\varphi} + i\frac{d\Delta y}{ie^{i\varphi}d\varphi}$$

or

$$\left|\frac{dz}{dp}\right| = \sqrt{\left(\left[\frac{d\zeta}{dp}\right] - \frac{d\Delta x}{d\varphi}\right)^2 + \left(\frac{d\Delta y}{d\varphi}\right)^2} \tag{29}$$

The velocity distribution at the surface of an arbitrary airfoil in cascade is therefore, by equations (18) and (26) to (29),

$$\frac{v_z}{V} = \frac{2\sqrt{\cos^2\lambda + \sinh^2 K}\left[\sin\left(\varphi - \lambda_K\right) - \sin\left(\varphi_T - \lambda_K\right)\right]}{\left(\sin^2\varphi + \sinh^2 K\right)\sqrt{\left(\left[\frac{dt}{dp}\right] - \frac{d\Delta x}{d\varphi}\right)^2 + \left(\frac{d\Delta y}{d\varphi}\right)^2}} \tag{30}$$

The numerator of this expression is seen to be dependent on, but the denominator independent of, the stream angle λ.

The pressure coefficient is given by Bernoulli's equation

$$P = 1 - \left(\frac{v_z}{V}\right)^2 \tag{31}$$

where P is the ratio of the local increment of static pressure over the pressure at which the velocity is the mean stream value V to the dynamic pressure $\frac{1}{2}\rho V^2$. Integration of this pressure coefficient around the airfoil section yields the lift coefficient defined by equation (23).

The expression for the ideal angle of attack may be noted. This angle is the mean relative stream angle for which the leading edge of the airfoil, corresponding to $\varphi = \varphi_N$ on the unit circle, is a stagnation point. It is obtained from the condition $v_p(\varphi) = 0$ in equation (26) as

$$\lambda_{K_i} = \frac{\varphi_N + \varphi_T - \pi}{2} \tag{32}$$

(The corresponding angle of attack measured from the "x-axis" chord line is given by equation (24a).) Conversely, for any stream angle λ, the front stagnation point is given by

$$\varphi_{N_s} = \pi + 2\lambda_K - \varphi_T \tag{33}$$

Superposition of solutions.- Equations (3) and (4) show that the sum of two CMF's is itself a CMF. Thus, as for isolated airfoils, the superposition of solutions for airfoils in cascade is permissible. Various types of superposition are possible because the solidity and stagger parameters K and β used with a resultant CMF need not be the same as either of these parameters used with the component CMF's. The use of superposition is implicit in the horizontal and vertical adjustment derived previously for an airfoil in cascade.

Equivalent flat-plate cascade.- The many useful results of reference 1, which are derived and presented on the conceptual basis of the equivalent cascade of flat plates, make it worth while to note some of the properties of the equivalent cascade. In general, the conformal transformation of a cascade of airfoils into a unit circle determines at the same time every possible cascade of flat plates into which the given cascade can be conformally transformed, with the spaces at $\pm\infty$ corresponding and equal. All such cascades of flat plates transform to the unit circle with the same locations for the points $p = \pm e^{K}$ corresponding to the points $\pm\infty$ in the cascade planes. The parameter K of the flat-plate transformation (equation (5)) is therefore fixed. Of the infinity of flat-plate cascades corresponding to the remaining parameter, namely, the stagger angle β, that one of which the stagger angle equals the zero-lift stream angle of the given cascade is by definition the equivalent cascade of flat plates. This stagger angle is Φ_{TK} by equation (20). Equation (21) then shows that the angle Φ_T corresponding to the trailing edge of the airfoil in cascade corresponds also to the trailing edge of the equivalent flat plate.

The solidity of the equivalent flat-plate cascade, as given by equation (8), is evidently somewhat larger than that of the given cascade. For a given stream angle λ, equation (20) shows that the circulation Γ and thus, by equation (23), the product σc_l are the same for the two cascades.

The velocity distribution in the airfoil cascade at one stream angle may be converted to a velocity distribution at any other stream angle by a knowledge of the equivalent cascade, because the ratio of the

velocities at two different stream angles is the ratio of the corresponding numerators in equation (30). Inasmuch as the constants of the numerator in equation (30) are the same for the given cascade and the equivalent cascade, the desired velocity ratio equals that for the equivalent cascade. This result is analogous to that for isolated airfoils and their equivalent flat plates. It is useful when the equivalent cascade can be easily determined to a satisfactory approximation (cf. reference 1). If the correspondence between an airfoil in cascade and its equivalent flat plate in cascade is known with sufficient accuracy, however, the CMF of the transformation $\Delta x(\varphi) + i\Delta y(\varphi)$ can be set up and the velocity distribution obtained directly by equation (30).

SOLUTION OF DIRECT POTENTIAL PROBLEM FOR CASCADES

The direct potential problem for cascades of airfoils is that of determining the general potential flow past, and in particular the velocity at the surface of, a known arbitrary airfoil in a cascade of given solidity σ and stagger angle β (fig. 1). The solution is analogous to that in reference 5 for isolated airfoils. The method is one of successive approximation, whereby an airfoil of which the CMF transformation to its "chord-line" cascade and hence to the unit circle is known is compared with the given airfoil to obtain an incremental CMF. The incremental CMF plus the known CMF yields an airfoil that may again be compared with the given airfoil, and so on.

The steps in the process are as follows:

Step 1: An airfoil in a cascade of stagger β and solidity σ is given and an initial airfoil is assumed, for which are known the CMF $\Delta x_0(\varphi)$, $\Delta y_0(\varphi)$, the angles φ_{N_0}, φ_{T_0} corresponding to the leading and trailing edges, the cascade parameter K_0, and the translation constant τ_0 - all adjusted for a cascade of the given stagger and solidity. The chordwise locations x_0 for this airfoil corresponding to a set of evenly spaced values of φ on the unit circle are calculated by equation (9).

Step 2: At the chordwise locations x_0, the differences $\delta y_1 = \Delta y_1 - \Delta y_0$ between the ordinates of the given airfoil and those of the assumed airfoil are obtained, graphically or otherwise. It is important that the given airfoil be located relative to the coordinate axes as shown in figure 1 and that, when the airfoil ordinates Δy_1 are obtained, the airfoil boundary be traversed (counterclockwise) in the same sense as is the extended chord line.

Step 3: The corresponding conjugate chordwise-displacement increments δx_1 are now calculated in accordance with equations (3) and (4). The slopes $d\delta x_1/d\phi$ and $d\delta y_1/d\phi$ are also computed by means of the corresponding derivative Fourier series. Details of this calculation are given in appendix A of reference 5.

Step 4: The first-approximation CMF, namely, $\Delta x_1 = \Delta x_0 + \delta x_1$ and $\Delta y_1 = \Delta y_0 + \delta y_1$, and the corresponding slopes $d\Delta x_1/d\phi$, $d\Delta y_1/d\Phi$ are now known. In conjunction with the constants K_0, Φ_{N_0}, Φ_{T_0}, and τ_0 of the initial airfoil, this CMF would, in general, determine an airfoil (equations (9) and (10)) of which the extremities (equations (11), (13), and (14)) would not add up to the desired chord ($c = 2nC$), although the stagger angle β (of the x-axis chord) is correct. The constants K_0, Φ_{N_0}, Φ_{T_0}, and τ_0 are therefore corrected by a horizontal stretching adjustment (equations (15), (16), and (17)) such that the resulting constants K_1, Φ_{N_1}, Φ_{T_1}, and τ_1 yield an airfoil of the desired chord.

Step 5: The new chordwise locations x_1 are calculated by equation (9) with the constants derived in step 4. The resulting airfoil, of coordinates x_1, Δy_1, is compared with the given airfoil. If the agreement is not satisfactorily close, steps 2 to 5 are repeated, all subscripts being advanced by one.

Step 6: If the agreement is close enough, the exact velocity distribution of the airfoil just derived (which is thus a close enough approximation to the velocity distribution of the given airfoil) is calculated as indicated in the section "Velocity and Pressure Distributions."

SOLUTION OF INVERSE POTENTIAL PROBLEM FOR CASCADES

As compared with the isolated airfoil, there are several possible variations of the inverse problem for cascades, depending on the over-all cascade data given in addition to the prescribed velocity distribution. These cascade data include the ultimate upstream and downstream flow angles considered as one quantity, the solidity σ, and the stagger angle β. Of these three quantities, it appears that two may be specified independently along with the prescribed velocity distribution.

The inverse problem for cascades can be solved by the method of comparison of surface potentials given in reference 5 for the case of the isolated airfoil. A numerical example, however, disclosed several difficulties of application. The over-all adjustment for one-to-one correspondence of the true and approximate potential curves was unduly laborious. Furthermore, the first exact velocity distribution obtained oscillated about the prescribed distribution through wide limits. This oscillation appeared to be caused by the somewhat indirect method of determining $\delta x(\varphi)$, resulting in inexact and oscillatory values for the derivatives $d\Delta x/d\varphi$, $d\Delta y/d\varphi$.

The more straightforward method of derivatives, namely, determining $d\Delta x/d\varphi$, $d\Delta y/d\varphi$ directly from the prescribed velocity distribution, was therefore resorted to. As remarked in reference 5, the method can be regarded as based on the use of the function $ip\frac{d(z - \zeta)}{dp}$. This function is single-valued and regular everywhere outside the unit circle; it approaches the limit zero as $p \to \infty$ and on the unit circle itself $p = e^{i\Phi}$ reduces to $\frac{d\Delta x}{d\Phi} + i\frac{d\Delta y}{d\Phi}$. If, therefore, these derivatives can be so determined as to satisfy the expression for the prescribed velocity distribution (equation (30)), the airfoil itself can then be obtained by a simple integration.

The determination of the derivatives can be made by successive approximation. The constants λ, F are fixed to satisfy approximately the over-all cascade

data previously mentioned. Inasmuch as the derivatives $d\Delta x/d\phi$, $d\Delta y/d\phi$ are of the same order of magnitude for the shapes to be dealt with, it is apparent from the structure of the radical in equation (30) that $d\Delta x/d\phi$ will exert a greater influence on the velocities over most of the airfoil than will $d\Delta y/d\phi$. To a given approximation, $d\Delta x/d\phi$ can therefore be solved for in terms of the prescribed velocity v_z and the data $d\Delta y/d\phi$, λ, and K of the previous approximation. A new $d\Delta y/d\phi$ can then be calculated as the function conjugate to this $d\Delta x/d\phi$; and λ, K can be corrected to serve as the basis for the next approximation.

The steps of the inverse process are outlined as follows:

Step 1: A velocity distribution expressed as a function of percentage chord or arc and the appropriate cascade data are given. The definition of the chord and the prescribed velocity distribution are taken as in reference 5. An initial airfoil is assumed, which is judged to produce approximately the desired conditions and for which the cascade CMF Δx_0, Δy_0 is known.

Step 2: If the given cascade data are the solidity σ and stagger angle β, a horizontal adjustment is applied to the CMF Δx_0, Δy_0 to achieve these values; that is, equations (15) and (16) with $S = 1$ are solved for K_0, Φ_{N_0}, and Φ_{Γ_0} with the given values of σ, β. Thence, equation (17) is solved for τ_0.

Step 3: The lift coefficient c_{l_0} corresponding to the prescribed velocity distribution is obtained approximately as the area under the curve of chordwise pressure distribution. A correction to this c_l, if necessary, is obtained by integrating the chordwise perpendicular pressure components of the prescribed distribution on the initial airfoil.[2] The required

[2]Equations (22) and (23) are dynamical equations, holding only for simply connected airfoils to which Bernoulli's equation applies. In order to preserve the consistency of the CMF equations for figure-eight contours, the circulation Γ can be approximated and equation (20) can be used directly.

stream angle λ_o for this c_{l_o} and σ is calculated from equations (23) and (20) by use of Φ_{T_o} and K_o of step 2. If the ultimate upstream and downstream flow angles are specified instead of the solidity, an extra relation between Γ and λ is known. If this relation and equation (23) are substituted in equation (20), an equation relating Φ_T, K, and σ results. This equation is solved simultaneously with equations (15) and (16) for Φ_{N_o}, Φ_{T_o}, K_o, and σ_o. These values then determine Γ_o, λ_o, and σ_o. A similar situation exists if the upstream and downstream angles and the solidity σ, instead of the stagger angle β, are specified.

Step 4: With the constants derived, the chordwise locations x_o are calculated by equation (9) for a set of evenly spaced φ-values.

Step 5: The first approximate derivative $d\Delta x_1/d\varphi$ is calculated by solution of equation (30) with the constants already derived, the prescribed velocity v_z/V corresponding to the chordwise locations x_o, and the initial $d\Delta y_o/d\varphi$.

Thus,

$$\frac{d\Delta x}{d\varphi} = \left[\frac{d\zeta}{dp}\right] \pm \sqrt{\left(\frac{v_n}{v_z}\right)^2 - \left(\frac{d\Delta y}{d\varphi}\right)^2} \qquad (34)$$

Two possible sets of values for $d\Delta x_1/d\varphi$ result from this calculation, depending on the sign of the square root in equation (34). It appears that for about one half the Φ-values, one set of $d\Delta x_1/d\varphi$ roots should be taken and for the other half, the other set. The resulting $d\Delta x_1/d\varphi$ should be of the right order of magnitude to lead to a real airfoil. Any imaginary roots that occur are replaced by the most favorable real values. (The assumption is that a real solution exists and that any imaginary values of $d\Delta x/d\varphi$ in equation (34) are the result of too poor an initial choice of $d\Delta y/d\varphi$.)

Step 6: The derivative $d\Delta y_1/d\varphi$ conjugate to the $d\Delta x_1/d\varphi$ of step 5 is calculated in accordance with the derivatives of equations (3) and (4). The functions $\Delta x_1(\varphi)$, $\Delta y_1(\varphi)$ are then obtained by integration. If the difference

$$\frac{d\delta x_1}{d\varphi} = \frac{d\Delta x_1}{d\varphi} - \frac{d\Delta x_0}{d\varphi}$$

is small, it may be more convenient, because of smaller required accuracy, to compute the increments $d\delta y_1/d\varphi$, δx_1, and δy_1 and add them to the corresponding values of the previous approximation.

Step 7: The horizontal adjustment of step 2 and the calculation of the stream angle λ_1, step 3, is made by using the first-approximation CMF derived in step 6.

Step 8: The chordwise locations x_1 are calculated as in step 4 by using the constants derived in step 7.

Step 9: The first approximate airfoil and its exact velocity distribution are calculated by equations (9), (10), and (30). If the velocity distribution is not satisfactorily close to that prescribed, the procedure is continued with step 5, all subscripts being advanced by one.

ILLUSTRATIVE EXAMPLES

Direct method.- As an illustration of the direct method, a cascade of solidity $\sigma = 1$ and blade angle $\beta = 45^\circ$ was assumed, together with the given airfoil section shown in figure 4, of which the ordinates are given in table I. In the resulting cascade arrangement (fig. 1) the flow is from right to left (compression action).

As a preliminary step, the direct CMF method (reference 5) was applied to the given section considered acting as an isolated airfoil. The resulting CMF and

transformation constants are given in tables II and III, respectively. It is remarked that the relatively poor initial approximation chosen, namely, a Joukowski airfoil of 6-percent camber and 12-percent thickness, necessitated three approximations before coincidence with the given airfoil (to a scale of chord length equal to 20 in.) was attained.

For the airfoil in cascade, the procedure outlined in the section "Solution of Direct Potential Problem for Cascades" was followed. In accordance with step 1 of the procedure, the initial approximation was taken as the cascade of chord lines of unit solidity and 45° blade angle. The initial CMF was thus $\Delta x_0 = \Delta y_0 = 0$. The parameter K_0, as determined from equation (8) with $\sigma_l = 1$ and $\beta = 45^\circ$, was 0.350. The chordwise locations x_0 were calculated from equation (9), with $\tau = \Delta x = 0$.

Steps 2 to 5 were then carried out. The resulting first approximate "airfoil" is shown in figure 4. The abscissas are the chordwise locations $x_1(\varphi)$ of the first approximation and the ordinates are those of the given airfoil at the chordwise locations $x_0(\varphi)$ of the initial approximation, which are indicated in figure 4. The first approximation is seen to have accomplished most of the required change from the chord line to the given airfoil. The resulting shape is not a physically real airfoil, however, because of the loop toward the trailing edge.

A second approximation gave results shown in figure 4. The agreement over most of the airfoil is good, although appreciable departures over the front upper surface and a slight loop near the trailing edge still remained. A third approximation removed practically all the remaining discrepancies. The points that were still perceptibly different are indicated in figure 4. A fourth approximation gave coincidence with the given airfoil to a scale of 20 inches for the length of chord.

The coincidence of the fourth approximate airfoil with the given airfoil was obtained for 24 points (besides the leading and trailing edges). These points correspond to 24 evenly spaced values of φ on the unit

circle. It is seen from figure 4 that the airfoil points are sparsely distributed on the front upper surface and rear lower surface, as compared with the rest of the airfoil. This distribution is due to the influence of the flat-plate transformation (equation (6)) in affecting the airfoil abscissas (equation (9)). Since the CMF was obtained in the form of 24-term Fourier expansions, it was thought that airfoil points obtained by interpolation from the derived CMF might show some waviness relative to the given airfoil in these regions. Five such interpolated points are given in table II and are shown in figure 4. The waviness appears to be negligible in this case. It is noted that any desired spacing of points on the airfoil could be obtained by working with appropriate unevenly spaced φ-points on the unit circle; however, the determination of $\Delta x(\varphi)$ from $\Delta y(\varphi)$ becomes more laborious.

The slight waviness in the Fourier expansions for $\Delta x(\varphi)$ and $\Delta y(\varphi)$ gives rise to greater oscillations in the corresponding derivative expansions for $d\Delta x/d\varphi$ and $d\Delta y/d\varphi$. In this example, the slopes were computed by harmonic synthesis of their Fourier expansions, and the results were smoothed out graphically to correspond to a faired curve through the 24 known values of Δx or Δy. The limits of oscillation of the derivative curves were small enough that no appreciable error was believed to be incurred in this process.[3]

---

[3]In extreme cases, where the higher harmonics in the $\Delta x(\varphi)$, $\Delta y(\varphi)$, curves are large, the oscillations of $d\Delta x/d\varphi$, $d\Delta y/d\varphi$ may lead to appreciable inaccuracy of the velocity distribution. It is possible, however, to solve initially for the derivatives $d\Delta x/d\varphi$, $d\Delta y/d\varphi$ instead of $\Delta x(\varphi)$, $\Delta y(\varphi)$ by working from the slopes dy/dx of the given airfoil, for

$$\frac{dy}{dx} = \frac{dy}{d(\xi + \Delta x)}$$

$$= \frac{d\Delta y/d\varphi}{\frac{d\xi}{d\varphi} + \frac{d\Delta x}{d\varphi}}$$

The resulting CMF's and the transformation constants for the airfoil in cascade are given in tables II and III, respectively. The column of values of k under "Cascade" in table II gives the values of the denominator in equation (30) for the velocity distribution. This factor does not change with angle of incidence of the flow.

The variation of lift coefficient with angle of attack for the cascade arrangement (equation (25)) was obtained as

$$c_l = 4.65 \sin (\alpha + 10°4')$$

where, it will be recalled, c_l is based on the mean velocity V and α is the angle between the mean velocity V and the chosen chord line. The lift-coefficient variation for the isolated airfoil was obtained as

$$c_l = 6.86 \sin (\alpha + 11°22')$$

---

with the result that

$$\frac{d\Delta y}{d\varphi} = \frac{dy}{dx}\left(\frac{d\zeta}{d\varphi} + \frac{d\Delta x}{d\varphi}\right)$$

Thus, to a given approximation, $d\Delta y/d\varphi$ can be determined from the known data of the previous approximation. To the given approximation, $d\Delta x/d\varphi$ is then the function conjugate to $d\Delta y/d\varphi$. The derivative $d\Delta y/d\varphi$ can then be determined to a better approximation, etc. In each approximation, an exact airfoil is determined by integration of $d\Delta x/d\varphi$, $d\Delta y/d\varphi$ (the integrated Fourier series are smoother than the original series). This method for the solution of the direct problem is the counterpart of the method of derivatives in the inverse problem. The accuracy of the derivatives $d\Delta x/d\varphi$, $d\Delta y/d\varphi$ thus determined depends primarily on the accuracy to which the airfoil slopes dy/dx are known. Corresponding remarks apply to the isolated-airfoil case, in which, however, the higher harmonics are usually of less magnitude.

The ratio of lift-curve slopes is thus $\frac{4.65}{6.86} = 0.678$ and the zero-lift angle for the cascade has been reduced by $1^\circ 18'$.

The equivalent cascade of flat plates has a stagger angle of $45^\circ - 10^\circ 4' = 34^\circ 56'$ and the solidity, as determined by equation (8) with $\beta = 34^\circ 56'$ and $K = 0.258$, is $\sigma_l = 1.19$. It may be noted that the ratio of lift-curve slope of the equivalent cascade to the isolated-plate value 2π is 0.624, which is about 8 percent less than the value for the given cascade. The corresponding ratio for the chord-line cascade ($\beta = 45^\circ$, $\sigma = 1$) is 0.844, or about 25 percent higher than that for the given cascade. If the equivalent cascade were based on the isolated-airfoil data, namely, $c_l = 1.0912$ and $\beta = 45^\circ - 11^\circ 22' = 33^\circ 38'$, the ratio of lift-curve slopes of the equivalent cascade is 0.655, which is a satisfactory approximation to the true value in this case.

The variation with lift coefficient of the various flow angles of the cascade as well as the over-all pressure-rise coefficient based on mean dynamic pressure is given in table IV. The values were calculated by means of the velocity triangle of the cascade (fig. 5). The deviations δ_N, δ_T of the upstream and downstream flow angles from the mean directions of the leading and trailing edges of the airfoil (fig. 5) are also given. The downstream flow angle λ_d is seen to remain essentially constant as the upstream flow angle is varied. In this respect, therefore, the cascade acts like one of infinite solidity. The deviation δ_T of the downstream flow from the direction of the trailing edge is large, however (about 18°).

The velocity distributions of both the isolated airfoil and the airfoil in cascade are shown for zero lift coefficient in figure 6 and for various other lift coefficients in figures 7 and 8. The velocity distributions at zero lift may be compared directly. Except near the leading and trailing edges, the velocities for airfoils in cascade are higher than the velocities for the isolated airfoil. This result may be ascribed to the constricting effect of two neighboring blades of the cascade on the streamlines between them. The velocity bump about 60 percent chord back on the upper

surface of the airfoil in cascade is probably caused by the sudden rate of change of flow area in this region due to the presence of the upper neighboring blade (fig. 5). At the leading edge, the velocity peak is lower for the airfoil in cascade than for the isolated airfoil, probably because of the effect of the lower adjacent airfoil in deflecting the upstream flow upward toward the nose. At the trailing edge, the velocity is lower for the airfoil in cascade than for the isolated airfoil, probably because the upper adjacent airfoil provides a divergent channel for the streamlines in this region.

The proper basis for comparison of velocity distributions of the isolated and cascade airfoils at lift coefficients other than zero is not clear. Because the cascade velocities (fig. 8) have been expressed as fractions of the mean velocity, the velocities toward the leading edge are higher than if the ultimate upstream velocity had been used as a base; whereas, toward the trailing edge, the velocities are lower than if the ultimate downstream velocities had been used as a base. The ultimate upstream and downstream velocities for the various lift coefficients are indicated by the horizontal lines in figure 8. In general, it appears that the adverse velocity gradients near the leading edge are less for the airfoil in cascade than for the isolated airfoil, whereas the adverse velocity gradients near the upper-surface trailing edge are greater in the cascade case.

The "ideal" velocity distributions, which produce a stagnation point at the chordwise extremity of the airfoil, are those for $c_{l_{isolated}} = 1.28$ and $c_{l_{cascade}} = 1.17$. It is seen that small velocity peaks are present on the lower-surface leading edge under these conditions. These peaks are removed in the isolated-airfoil case at $c_l = 1.30$ and for the cascade at about $c_l = 1.30$ without producing peaks on the upper surface. The incidence of the upstream flow relative to the chord line is $15^{\circ}24'$ in the case of $c_l = 1.30$.

The four approximations in this example were carried out without any attempt at picking off the ordinates in order to anticipate the resulting change in chordwise

location. It may be expected that, when more favorable initial approximations than the chord line are available and with some experience in anticipating changes in chordwise locations, no more than two approximations will be necessary for accurate results - that is, results less than 1 percent in error.

Finally, it may be noted that the CMF derived for the given airfoil can be used as a good initial approximation not only for similar airfoils in compressor action but also for airfoils in turbine action. For this latter application, the airfoil would be drawn with the camber on the same side of the chord line as in figure 1. The flow is then from left to right; that is, λ is increased by 180°. This procedure appears more favorable numerically than drawing the airfoil with the camber on the other side of the chord line, which would maintain the flow from right to left.

Inverse method.- In order to illustrate the inverse method for cascades, the velocity distribution at $c_l = 1.3$ of the airfoil just analyzed was modified as indicated in figure 9. The corresponding prescribed pressure distribution is constant up to 50 percent chord and thereafter increases linearly to the trailing edge. The prescribed cascade data were taken as $\sigma = 1$, $\beta = 45°$. The ultimate upstream and downstream angles, or blade circulation, were expected to be about the same as those for the initial airfoil in cascade at $c_l = 1.3$.

The procedure already outlined was followed. The initial airfoil was chosen as the one just analyzed by the direct method (fig. 10). The CMF and associated constants of the initial airfoil are given in tables II and III. The initial CMF was actually taken as 1.145 times the values of table II, because the use of the method of potentials had indicated this factor as a preliminary over-all adjustment. The chordwise locations of table II were consequently corrected. The initial lift coefficient was taken as the area enclosed by the prescribed $\left(\frac{v}{V}\right)^2$-curve, namely, $c_l = 1.26$.

The first-approximation $d\Delta x_1/d\varphi$ was thereupon calculated from equation (34) and plotted in figure 11. Except at $\varphi = 15°$, this curve represents the solution

of equation (34) with the negative square root for $30^\circ \leq \varphi \leq 180^\circ$ and the solution with the positive root for the remaining φ-values. At $\varphi = 15^\circ$, the calculated roots were complex. The $\frac{d\delta x_1}{d\Phi}$-curve was therefore faired through $\varphi = 15^\circ$ to complete the specification of $d\Delta x_1/d\Phi$. The increment

$$\frac{d\delta x_1}{d\Phi} = \frac{d\Delta x_1}{d\Phi} - \frac{d\Delta x_0}{d\Phi}$$

was then used to calculate the first-approximation conjugate increment

$$\frac{d\delta y_1}{d\Phi} = \frac{d\Delta y_1}{d\Phi} - \frac{d\Delta y_0}{d\Phi}$$

and the incremental airfoil CMF $\delta x_1 + i\delta y_1$. The Runge 24-point schedule (see appendix A of reference 5) was used for these calculations. The horizontal adjustment then applied to this CMF was such as to maintain $\sigma = 1$, $\theta = 45^\circ$ (with respect to the chord chosen for the initial airfoil, the so-called x-axis chord). The first approximate CMF is listed in table V and the associated constants in table VI. The first approximate airfoil is shown in figure 10 and its exact velocity distribution, for $c_l = 1.26$, in figure 9. The cascade flow angles for the derived sections are given in table VII.

The changes in velocity distribution and airfoil contour and position from their initial values are seen to be considerable. The mean line of the derived section is reflexed toward the trailing edge, probably because of the influence on the "mean" streamline of the vorticity toward the leading edge on the upper neighboring airfoil (fig. 5). The maximum thickness of the derived section has been increased from 10 percent to about 15 percent. Furthermore, the section as a whole has been rotated about $2\frac{1}{2}^\circ$, with the result that the cascade blade angle, although equal to 45° as measured from the initial or x-axis chord line, is about 42.5° as measured from the "longest-line" chord in the derived airfoil. A slight change in cascade solidity is similarly brought about.

A second approximation to the prescribed velocity distribution was next carried out, with the initially chosen chord maintained as the "chord" of the derived airfoils. It was evident that the poor first approximation on the upper-surface leading edge, particularly for $\varphi = 15^\circ$, was due originally to fairing the $\frac{d\delta x_1}{d\varphi}$-curve through this point too smoothly. The resulting value of $d\Delta x_1/d\varphi$ was not the best possible real value, which is in this case the one that makes the velocity on the airfoil at this point as high as possible or, from equation (30),

$$\left(\frac{d\Delta x}{d\varphi}\right)_{\varphi=15^\circ} = \left[\frac{dt}{dp}\right]_{\varphi=15^\circ}$$

This value was therefore given to $\left(\frac{d\Delta x_2}{d\varphi}\right)_{\varphi=15^\circ}$ for the second approximation with the remaining values calculated as in the first approximation. The incremental derivative $\frac{d\delta x_2}{d\varphi} = \frac{d\Delta x_2}{d\varphi} - \frac{d\Delta x_1}{d\varphi}$ thus obtained is shown in figure 11. The conjugate function $d\delta y_2/d\varphi$ calculated therefrom is shown in figure 11. The oscillatory nature of $d\delta y_2/d\varphi$ is caused by the large magnitude of the higher harmonics in the Fourier series for $d\delta x_2/d\varphi$. The δy_2-function, as obtained by synthesis of the integrated Fourier series for $d\delta y_2/d\varphi$, displayed very little oscillation. The slopes of the smoothly drawn δy_2-curve were therefore measured graphically at all but the $\varphi = 0^\circ$, 15° points. The $\frac{d\delta y_2}{d\varphi}$-curve thus obtained is seen from figure 11 to be a mean curve through the calculated $\frac{d\Delta y_2}{d\varphi}$-values. This curve was used in the calculation of the second-approximation velocity distribution. Use of the measured values of $d\delta y_2/d\varphi$ as compared with the calculated values removed an oscillation of, at most, ±2 percent in the velocity distribution. Any error in measurement of the

$\frac{d\delta y_2}{d\theta}$-slopes would therefore produce the quite negligible error of a small fraction of ±2 percent.

The second approximation was carried out for $c_l = 1.26$. The resulting CMF and associated constants are given in tables V and VI. The second-approximation airfoil and its exact velocity distribution are shown in figures 10 and 9, respectively. The velocity distribution is seen to be converging satisfactorily to the prescribed values, though perhaps not so rapidly as would be the case for an isolated airfoil. The tendency toward formation of a velocity hump about 60 percent chord back on the upper surface is seen. As previously mentioned for the direct method, this effect may be due to the sudden constriction of the stream caused by the forward part of the upper neighboring airfoil (fig. 5). The second approximate airfoil differs from the first approximate airfoil mainly in having greater thickness toward the nose and less over-all camber. The greater thickness toward the nose is evidently the consequence of a higher required velocity on the upper surface at the leading edge. The reduced over-all camber appears to be caused by the necessity of a more constricted stream over the rear upper surface (higher required velocities). The forward half of the upper neighboring profile (fig. 5) shifts downward to accomplish this constriction.

A sharp cusp, possibly even a slight, physically impossible loop, is evident at the trailing edge. Apparently, the prescribed velocity in this region is close to being unattainable with a physically real airfoil. The necessity of as sharp a cusp as possible at the trailing edge seems definite.

From the practical point of view, two approximations are considered sufficient in this case. The necessary modifications of the initial airfoil to produce the modified velocity distribution are clearly indicated. The results of this and the preceding example can now be used as good initial approximations in further modifications either of airfoil shape or of velocity distribution, or, to a lesser extent, of cascade geometry.

CONCLUSIONS

1. The direct and inverse Cartesian mapping function (CMF) methods already used for isolated airfoils can be applied directly and analogously to the cascade case.

2. The cascade problem represents a more severe test of the CMF method than does the isolated-airfoil problem. Although the convergence of the successive approximations is slower in the case of cascades than in the corresponding isolated-airfoil cases, the numerical work for a given accuracy is considerably less than hitherto required, at least for cascade solidities near unity.

Langley Memorial Aeronautical Laboratory
National Advisory Committee for Aeronautics
Langley Field, Va.

REFERENCES

1. Weinig, F.: Die Strömung um die Schaufeln von Turbomaschinen. Johann Ambrosius Barth (Leipzig), 1935.

2. Collar, A. R.: The Flow of a Perfect Fluid through Cascades of Aerofoils. Jour. R.A.S., vol. XLV, no. 365, May 1941, pp. 183-213.

3. Theodorsen, T., and Garrick, I. E.: General Potential Theory of Arbitrary Wing Sections. NACA Rep. No. 452, 1933.

4. Garrick, I. E.: On the Plane Potential Flow past a Symmetrical Lattice of Arbitrary Airfoils. NACA ARR No. 4A07, 1944.

5. Mutterperl, William: The Conformal Transformation of an Airfoil into a Straight Line and Its Application to the Inverse Problem of Airfoil Theory. NACA ARR No. L4K22a, 1944.

6. von Kármán, Th., and Burgers, J. M.: General Aerodynamic Theory - Perfect Fluids. Application of the Theory of Conformal Transformation to the Investigation of the Flow around Airfoil Profiles. Vol. II of Aerodynamic Theory, div. E, ch. II, pt. B. W. F. Durand, ed., Julius Springer (Berlin), 1935, p. 91.

TABLE I.- AIRFOIL ORDINATES, DIRECT PROCESS

[Stations and ordinates in percent of airfoil chord]

Upper surface		Lower surface	
Station	Ordinate	Station	Ordinate
0	0	0	0
.23	.97	.77	-.43
.44	1.24	1.06	-.44
.88	1.66	1.62	-.46
2.03	2.63	2.97	-.37
4.43	4.17	5.57	-.13
6.87	5.44	8.13	.18
9.34	6.56	10.66	.46
14.34	8.46	15.66	1.08
19.36	9.98	20.62	1.64
24.44	11.24	25.56	2.16
29.55	12.20	30.45	2.60
34.64	12.90	35.36	2.96
39.72	13.39	40.28	3.29
44.82	13.64	45.18	3.58
49.96	13.65	50.04	3.91
55.07	13.37	54.93	4.23
60.17	12.78	59.83	4.48
65.26	11.92	64.74	4.68
70.30	10.81	69.70	4.77
75.32	9.53	74.68	4.67
80.29	8.04	79.71	4.39
85.23	6.40	84.77	3.94
90.17	4.56	89.83	3.10
95.10	2.57	94.90	1.89
100	0	100	0

NATIONAL ADVISORY
COMMITTEE FOR AERONAUTICS

TABLE II.- CMF's FOR ISOLATED AIRFOIL AND FOR AIRFOILS IN CASCADE NATIONAL ADVISORY COMMITTEE FOR AERONAUTICS

φ (radians)	Isolated						Cascade					
	Δx	Δy	$\frac{d\Delta x}{d\varphi}$	$\frac{d\Delta y}{d\varphi}$	x	k	Δx	$\frac{\Delta y}{w}$	$\frac{d\Delta x}{d\varphi}$	$\frac{d\Delta y}{d\varphi}$	$\frac{x}{w}$	k
0 × $\frac{\pi}{12}$	-0.125	0.027	-0.137	0.165	0.987	0.197	-0.729	-0.165	-0.316	1.696	0.765	0.366
1	-.152	.076	-.0655	.208	.923	.372	-.610	-.029	1.028	1.024	.982	.181
2	-.156	.133	.0130	.220	.810	.528	-.346	.008	.800	.0408	.989	.158
3	-.139	.188	.0985	.205	.653	.645	-.190	.005	.466	-.0627	.927	.610
4	-.105	.235	.175	.160	.462	.721	-.0856	-.005	.320	-.110	.848	.826
5	-.0516	.266	.228	.0770	.252	.760	-.0123	-.013	.230	-.14	.762	1.096
6	.0105	.273	.244	-.0250	.0314	.778	.0407	-.026	.170	-.14	.667	1.289
7	.0744	.258	.228	-.124	-.187	.766	.0776	-.036	.122	-.14	.560	1.392
8	.122	.216	.160	-.196	-.403	.750	.113	-.049	.084	-.14	.436	1.386
9	.146	.160	.0553	-.214	-.604	.685	.122	-.060	.0691	-.16	.273	1.264
10	.148	.101	-.0401	-.200	-.776	.567	.146	-.074	.0281	-.28	.0530	1.046
11	.127	.051	-.116	-.162	-.906	.394	.0739	-.096	-.557	.0480	-.325	.810
12	.0867	.014	-.180	-.107	-.982	.192	-.0042	-.047	.293	.896	-.864	.354
13	.0360	.001	-.216	.0245	-.998	.0654	.227	-.012	1.087	-.304	-.982	.174
14	-.0121	.026	-.122	.149	-.936	.412	.382	-.071	.10	-.745	-.853	.603
15	-.0235	.067	.0278	.146	-.774	.745	.371	-.113	-.04	-.46	-.744	.796
16	-.0042	.092	.105	.0497	-.529	.963	.356	-.149	-.12	-.36	-.638	1.023
17	.0223	.092	.0693	-.0596	-.259	1.031	.303	-.176	-.18	-.30	-.644	1.176
18	.0319	.074	.006	-.0682	.0528	1.005	.257	-.202	-.235	-.28	-.448	1.247
19	.0317	.057	-.003	-.0646	.335	.964	.177	-.225	-.28	-.27	-.354	1.256
20	.0277	.032	-.0458	-.101	.594	.829	.0866	-.247	-.395	-.24	-.247	1.144
21	.0063	.009	-.105	-.0850	.799	.616	-.0484	-.264	-.669	-.14	-.124	.974
22	-.0294	-.007	-.168	-.0350	.937	.347	-.216	-.273	-.794	.03	.0499	.798
23	-.0788	-.006	-.206	.0721	.996	.0966	-.490	-.258	-1.218	.631	.316	.677
							Interpolated					
0.5							-.720	-.085	.65	1.65	.914	.265
10.6							.130	-.087	-.24	-.27	-.107	.963
11.6							.010	-.082	-.36	.62	-.598	.590
22.5							-.340	-.270	-1.01	.16	.166	.684
23.6							-.635	-.219	-1.15	1.30	.524	.470

TABLE III.- TRANSFORMATION CONSTANTS FOR TABLE II

	σ	β (deg)	K	φ_N	φ_T	β_T	$\frac{dc_l}{d\alpha}$	τ	R
Cascade	1	45°	0.258	22°57'	190°0'	10°4'	4.65	0.197	------
Isolated	0	0	∞	-10°10'	191°22'	11°22'	6.86	.0209	1.0912

TABLE IV.- VARIATION OF FLOW ANGLES WITH BLADE LOADING

c_l	α	λ	λ_u	λ_d	$\Delta\lambda$	δ_N	δ_T	$P_u - P_d$
Cascade								
0	-10°4'	34°56'	34°56'	34°56'	0	32°34'	17°3'	0
.5	-3°54'	41°6'	46°6'	35°19'	10°47'	21°24'	17°26'	.329
1.0	2°21'	47°21'	55°27'	35°43'	19°44'	12°3'	17°50'	.734
1.17 (ideal)	4°31'	49°31'	58°23'	35°51'	22°32'	9°7'	17°58'	.891
1.3	6°10'	51°10'	60°24'	35°54'	24°30'	7°6'	18°1'	1.013
1.5	8°45'	53°45'	63°27'	36°12'	27°15'	4°3'	18°19'	1.214
2.0	15°25'	60°25'	70°11'	36°52'	33°19'	-2°41'	18°59'	1.741
Isolated								
0	-11°22'					33°52'	15°45'	
.5	-7°11'					29°41'	19°56'	
1.0	-2°59'					25°29'	24°8'	
1.28 (ideal)	-0°36'					23°6'	26°31'	
1.5	1°16'					21°14'	28°23'	
2.0	5°36'					16°54'	32°43'	

TABLE V.- CASCADE CMF BY INVERSE METHOD

First approximation

φ	Δx_1	$\frac{\Delta y_1}{\pi}$	$\frac{d\Delta x_1}{d\varphi}$	$\frac{d\Delta y_1}{d\varphi}$	$\frac{x_1}{\pi}$	k_1	v_{z_1}/V (c_l = 1.26)	
0 × $\frac{\pi}{12}$	-0.717	-0.241	-0.411	1.673	0.768	0.344	1.598	Upper surface
1	-.621	-.114	.987	1.028	.989	.161	1.248	
2	-.377	-.0798	.701	-.0011	.922	.204	.737	
3	-.258	-.0338	.324	-.0440	.904	.599	.803	
4	-.195	-.0873	.184	-.0176	.810	.936	.819	
5	-.155	-.0826	.124	-.0322	.712	1.104	.829	
6	-.134	-.0902	.0862	.0342	.607	1.366	.832	Lower surface
7	-.115	-.0858	.0694	.0201	.494	1.430	.834	
8	-.0973	-.0816	.0666	.129	.364	1.359	.832	
9	-.0831	-.0716	.0933	.0547	.203	1.228	.839	
10	-.0550	-.0566	.186	.248	-.0158	.979	.840	
11	.0016	-.0312	.213	.176	-.356	.691	.793	
12	.0747	-.0125	.575	.502	-.837	.319	.703	
13	.336	.0021	1.216	-.418	-.974	.197	.614	
14	.534	-.0695	.265	-.958	-.826	.587	.809	
15	.545	-.130	.0172	-.663	-.706	.879	.916	
16	.532	-.183	-.128	-.533	-.597	1.073	1.018	Upper surface
17	.468	-.223	-.210	-.441	-.507	1.191	1.104	
18	.409	-.261	-.257	-.410	-.414	1.232	1.184	
19	.306	-.291	-.366	-.373	-.327	1.194	1.268	
20	.188	-.322	-.464	-.272	-.230	1.055	1.386	
21	.0398	-.343	-.624	-.225	-.112	.936	1.442	
22	-.162	-.357	-.919	.0363	.0527	.748	1.533	
23	-.460	-.341	-1.245	.624	.317	.563	1.551	

TABLE V.- CASCADE CMF BY INVERSE METHOD - Concluded

Second approximation

φ	Δx_2	$\frac{\Delta y_2}{\pi}$	$\frac{d\Delta x_2}{d\varphi}$	$\frac{d\Delta y_2}{d\varphi}$	$\frac{x_2}{\pi}$	k_2	$\frac{v_{z_2}/V}{(c_l = 1.26)}$	
$0 \times \frac{\pi}{12}$	-0.676	-0.212	-0.220	1.269	0.802	0.334	1.568	Upper surface
1	-.648	-.120	.280	.989	1.0	.124	1.508	
2	-.494	-.0514	.788	.236	.957	.205	.776	Lower surface
3	-.310	-.0418	.384	.0401	.896	.575	.841	
4	-.238	-.0417	.226	.0130	.804	.908	.842	
5	-.162	-.0409	.152	-.0188	.717	1.166	.843	
6	-.129	-.0425	.116	.0258	.615	1.332	.842	
7	-.0801	-.0392	.0986	-.00817	.511	1.394	.844	
8	-.0502	-.0363	.0761	.0910	.365	1.369	.832	
9	-.0130	-.0318	.124	.00128	.231	1.198	.845	
10	.0350	-.0233	.216	.1300	.0197	.954	.843	
11	.112	-.0208	.178	-.00737	-.319	.681	.790	
12	.163	-.00877	.364	.390	-.856	.318	.691	
13	.385	.00050	1.044	-.459	-.974	.188	.657	
14	.554	-.0732	.0857	-.948	-.828	.544	.862	
15	.532	-.131	-.135	-.634	-.716	.706	.996	
16	.503	-.179	-.240	-.408	-.611	.973	1.104	
17	.423	-.214	-.294	-.376	-.524	1.092	1.184	Upper surface
18	.364	-.247	-.359	-.345	-.431	1.135	1.262	
19	.250	-.274	-.418	-.306	-.343	1.120	1.327	
20	.150	-.296	-.454	-.241	-.244	1.079	1.343	
21	-.0010	-.316	-.600	-.219	-.126	.908	1.456	
22	-.180	-.329	-.944	.0611	.0440	.730	1.531	
23	-.498	-.310	-1.246	.653	.308	.555	1.528	

TABLE VI.- ASSOCIATED CONSTANTS FOR CMF OF TABLE V

$[\sigma = 1, \quad \beta = 45^\circ]$

Approximation	σ (a)	β (a)	K	Φ_N	Φ_T	β_T (a)	dc_l/da	τ
1	1.001	42°30'	0.247	21°10'	189°46'	7°5'	4.69	0.167
2	1.001	41°30'	.237	14°17'	189°40'	5°17'	4.75	.172

[a]Measured from "longest-line" chord of airfoil.

TABLE VII.- CASCADE FLOW ANGLES FOR DERIVED AIRFOIL SECTIONS

Approximation	c_l	α (a)	λ	λ_u	λ_d	$\Delta\lambda$	δ_N	δ_T	$P_u - P_d$
1	1.26	8°30'	51°	60°4'	36°18'	23°46'	6°32'	-7°53'	0.98
2	1.26	10°6'	51°36'	60°31'	37°4'	23°27'	-8°42'	-7°56'	.99

[a]Measured from "longest-line" chord of airfoil.

Fig. 1

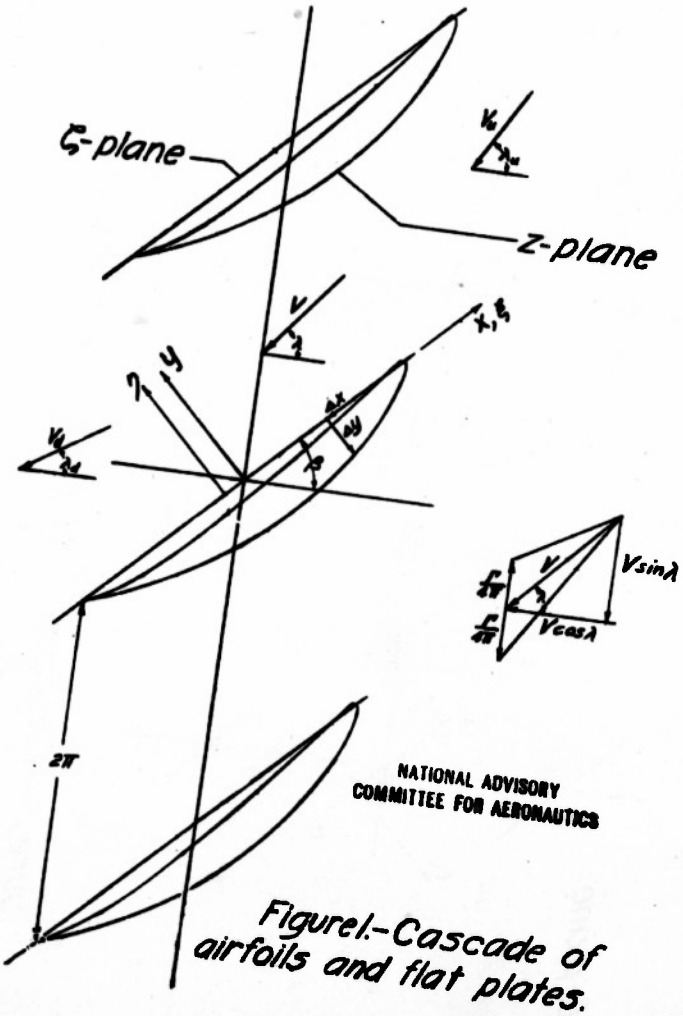

NATIONAL ADVISORY
COMMITTEE FOR AERONAUTICS

Figure 1.- Cascade of airfoils and flat plates.

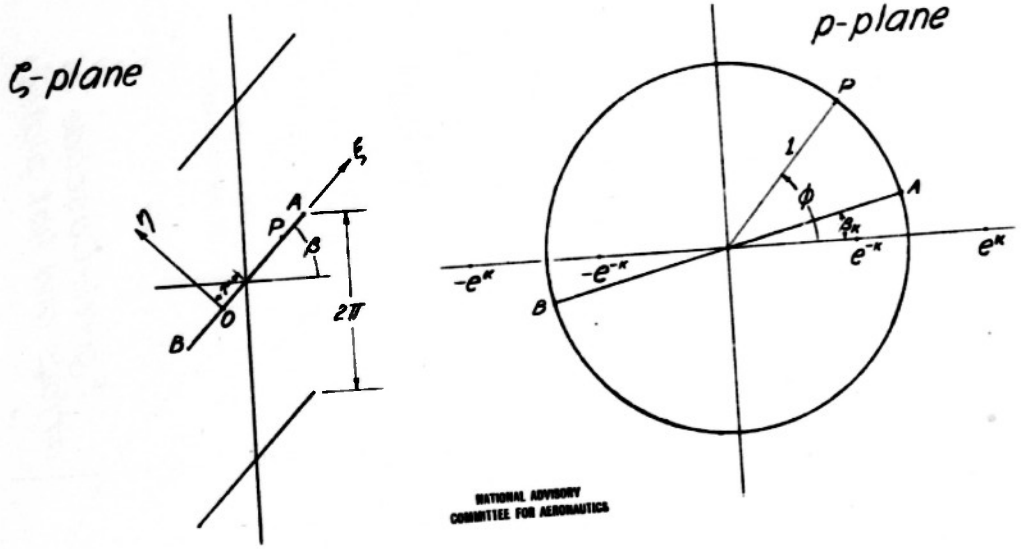

Figure 2.— Cascade flat-plate transformation.

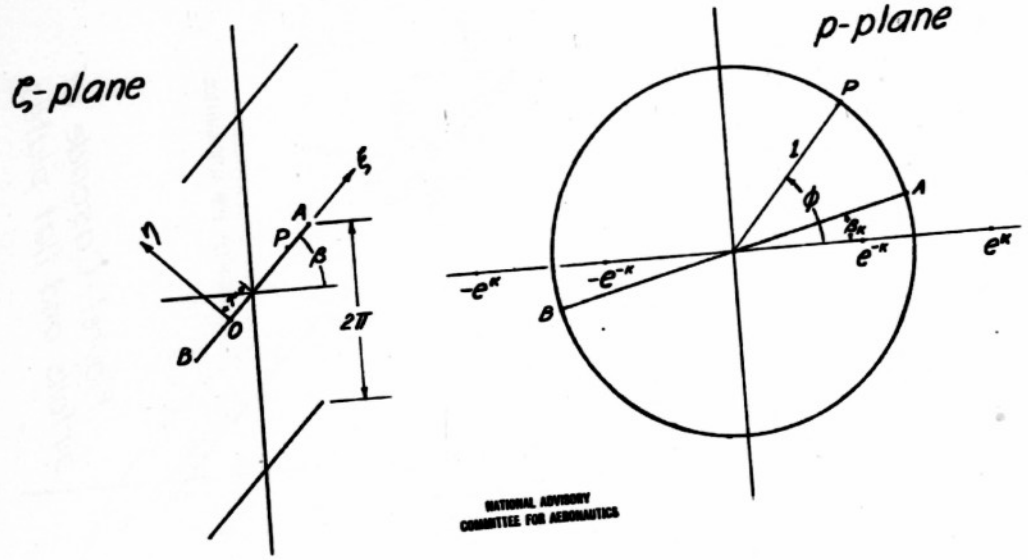

Figure 2.— Cascade flat-plate transformation.

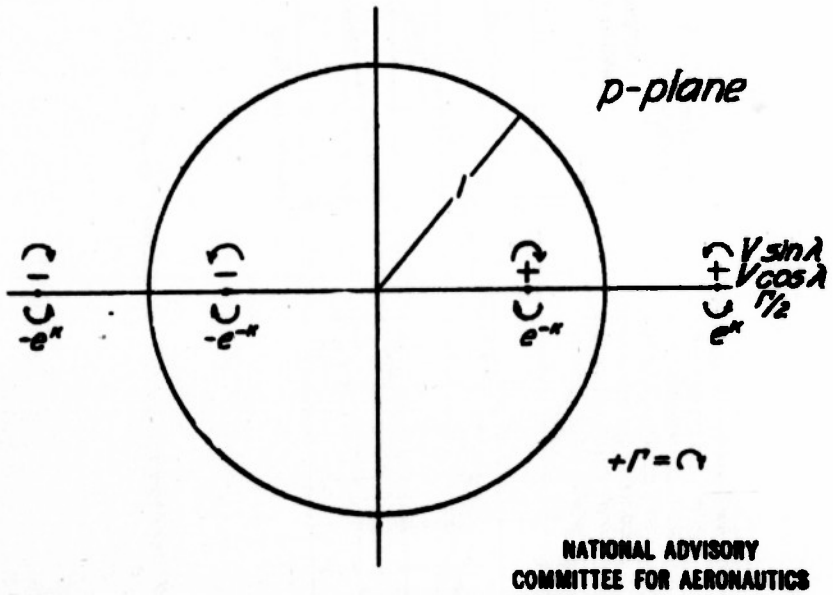

Figure 3.— Source-vortex system for cascade flow.

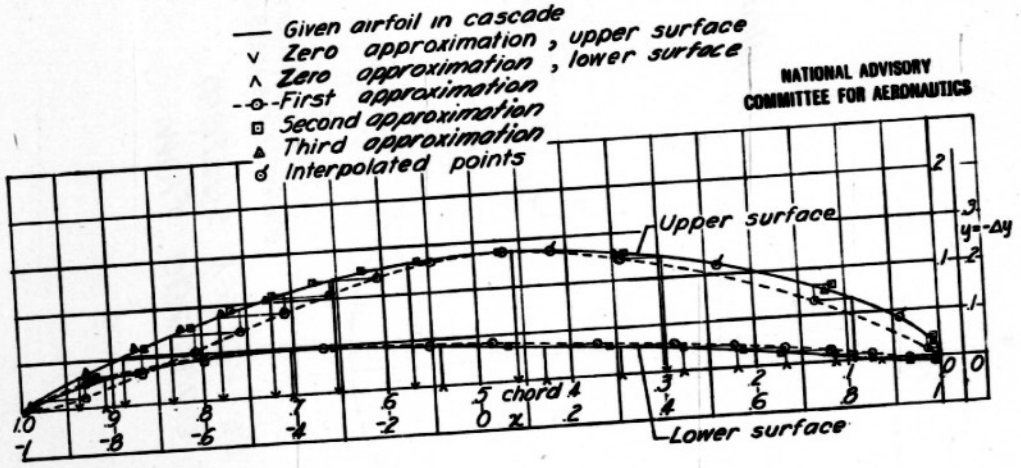

Figure 4.— Direct CMF method for airfoil in cascade. $\beta=45°$, $\sigma=1$.

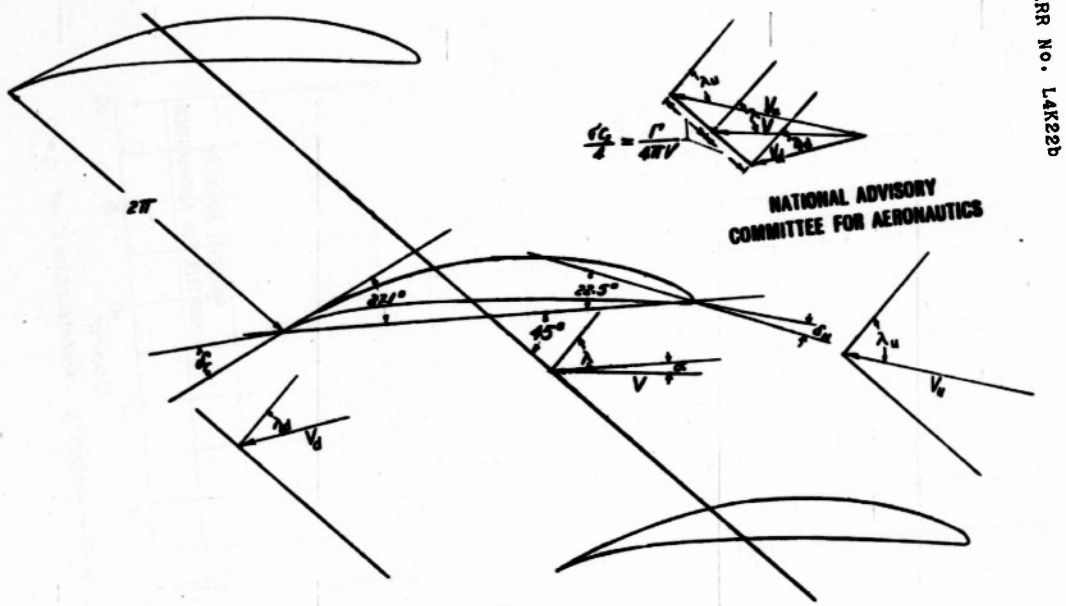

Figure 5.—Flow angles for cascade of airfoils.

Fig. 6

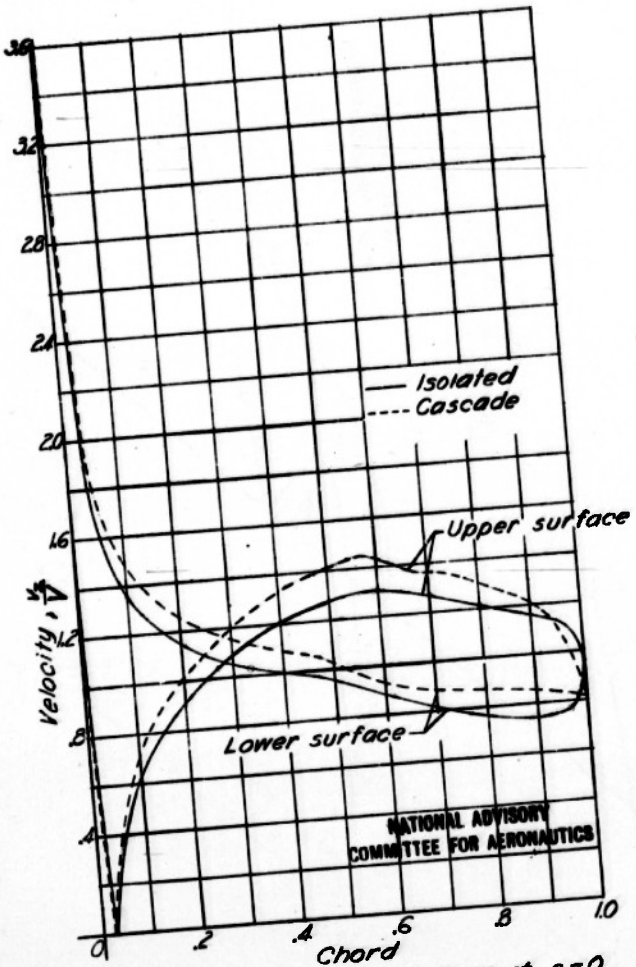

Figure 6.— Velocity distributions at $\alpha_i = 0$.

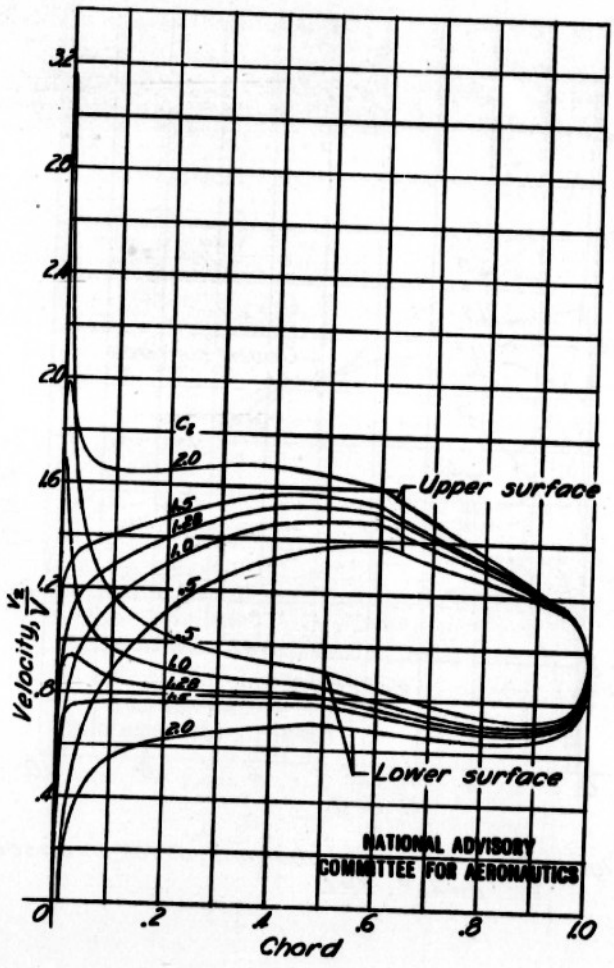

Figure 7.— Velocity distributions, isolated airfoil.

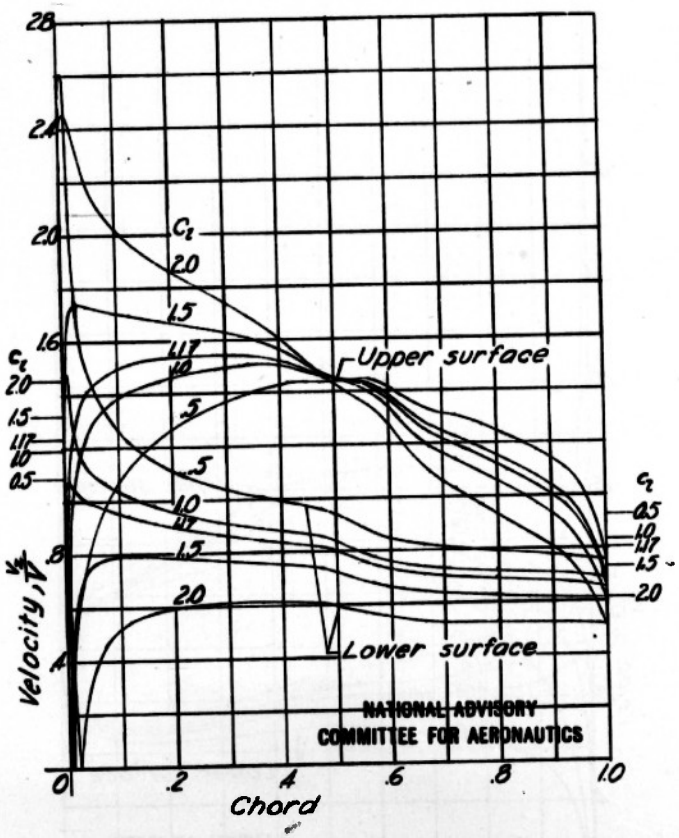

Figure 8.—Velocity distributions, airfoil in cascade. $\beta = 45°$, $\sigma = 1$.

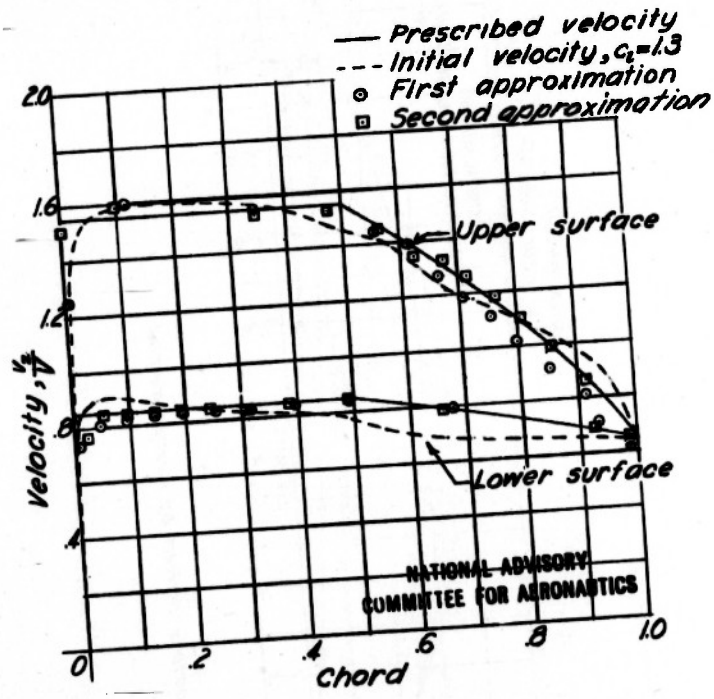

Figure 9.— Velocity distributions in cascade by inverse method.

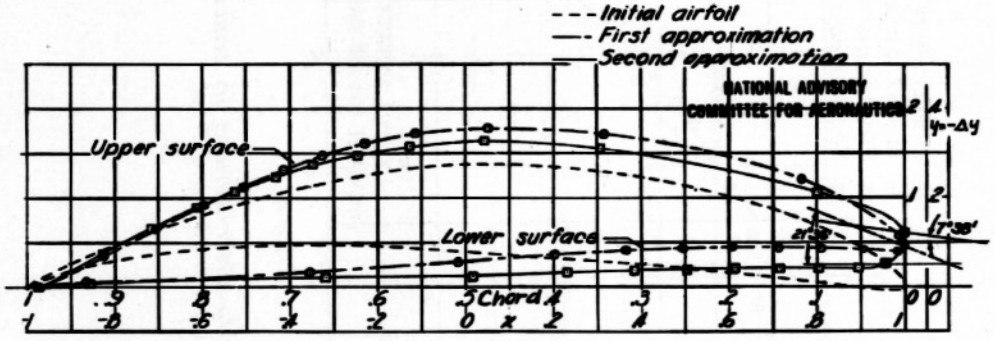

Figure 10.— Cascade airfoils derived by inverse method.

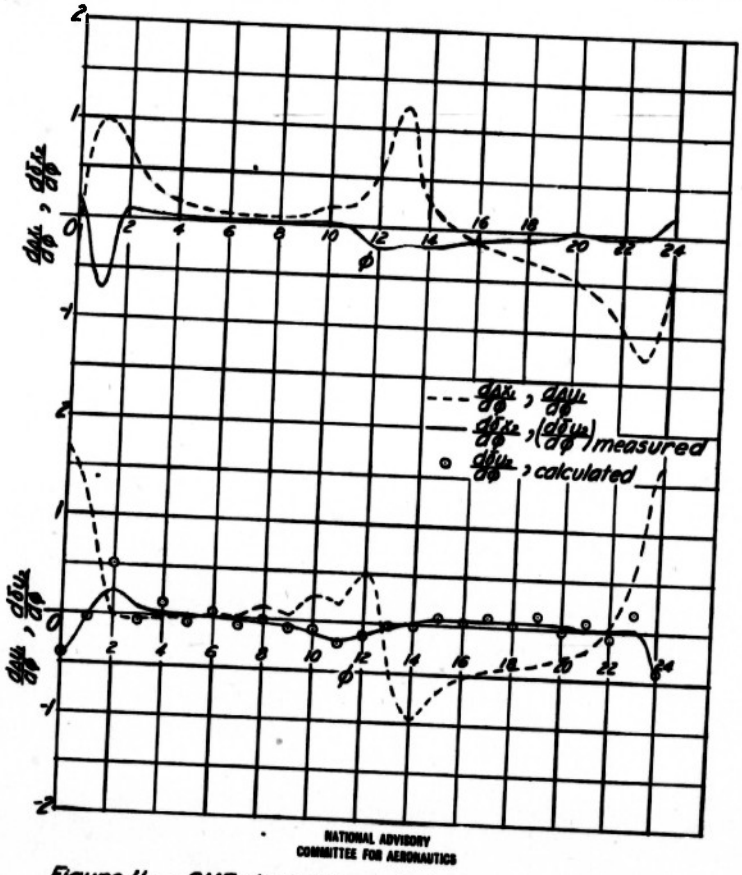

Figure 11.— CMF derivatives by inverse method for airfoils in cascade.

REEL - C

168

A.T.I.

6409

TSDIN FORM 69 (13 MAR 47)

Mutterperl, W

AUTHOR(S)

DIVISION: Aerodynamice (2)
SECTION: Wings and Airfoils (6)
CROSS REFERENCES: Airfoils - Caecades (08000); Flow research - Methods (40950); Flow around bodies (40450)

9 6-7 P01/03

ATI- 6409
ORIG. AGENCY NUMBER
ARR L4K22b
REVISION

AMER. TITLE: A eolution of the direct and inverse potential problems for arbitrary cascadee of airfoils

FORG'N. TITLE: *Cascades (Fluid Dynamics)

OVER

U

ORIGINATING AGENCY: National Advisory Committee for Aeronautics, Washington, D. C.

TRANSLATION:

COUNTRY	LANGUAGE	FORG'N.CLASS	U. S.CLASS.	DATE	PAGES	ILLUS.	FEATURES
U.S.	Eng.		Unclaee.	Dec'44	50	18	tsblee, diagre, graphs

ABSTRACT

Methods are given of determining the potential flow past an arbitrary cascade of airfoile and the inverse problem of determining an airfoil having a prescribed velocity dietribution in cascade. Reeulte indicate that Cartesian mapping function method may be eatiefactorily extended to include caecades. Numerical calculation for computing caecades by Carteeian mapping function method is coneiderably greater than for single airfoils but much leee than hitherto required for caecades. Detailed resulte are presented graphically.

NOTE: Requests for copies of this report muet be addressed to: N.A.C.A., Washington, D. C.

TSDIN FORM 69 (13 OCT 47)

Mutterperl, W

AUTHOR(S)

DIVISION: Aerodynamics (2)
SECTION: Wings and Airfoils (6)
CROSS REFERENCES: Airfoils - Cascades (08000); Flow research - Methods (40950); Flow around bodies (40450)

ATI- 6409
ORIG. AGENCY NUMBER
ARR L4K22b
REVISION

AMER. TITLE: A solution of the direct and inverse potential problems for arbitrary cascades of airfoils

FORG'N. TITLE:

ORIGINATING AGENCY: National Advisory Committee for Aeronautics, Washington, D. C.

TRANSLATION:

COUNTRY	LANGUAGE	FORG'N CLASS	U. S. CLASS.	DATE	PAGES	ILLUS.	FEATURES
U.S.	Eng.		Unclass.	Dec '44	50	18	tables, diagrs, graphs

ABSTRACT

Methods are given of determining the potential flow past an arbitrary cascade of airfoils and the inverse problem of determining an airfoil having a prescribed velocity distribution in cascade. Results indicate that Cartesian mapping function method may be satisfactorily extended to include cascades. Numerical calculation for computing cascades by Cartesian mapping function method is considerably greater than for single airfoils but much less than hitherto required for cascades. Detailed results are presented graphically.

NOTE: Requests for copies of this report must be addressed to: N.A.C.A., Washington, D. C.